Translational Science

Cancer Research

Meflin-Positive Cancer-Associated Fibroblasts Inhibit Pancreatic Carcinogenesis

Yasuyuki Mizutani[1,2], Hiroki Kobayashi[1,3], Tadashi Iida[1,2], Naoya Asai[1,4], Atsushi Masamune[5], Akitoshi Hara[1], Nobutoshi Esaki[1], Kaori Ushida[1], Shinji Mii[1], Yukihiro Shiraki[1], Kenju Ando[1], Liang Weng[1], Seiichiro Ishihara[6], Suzanne M. Ponik[7], Matthew W. Conklin[7], Hisashi Haga[6], Arata Nagasaka[8], Takaki Miyata[9], Makoto Matsuyama[10], Tomoe Kobayashi[10], Tsutomu Fujii[11], Suguru Yamada[12], Junpei Yamaguchi[13], Tongtong Wang[3], Susan L. Woods[3], Daniel Worthley[3], Teppei Shimamura[14], Mitsuhiro Fujishiro[2], Yoshiki Hirooka[15], Atsushi Enomoto[1], and Masahide Takahashi[1,4]

Abstract

Cancer-associated fibroblasts (CAF) constitute a major component of the tumor microenvironment. Recent observations in genetically engineered mouse models and clinical studies have suggested that there may exist at least two functionally different populations of CAFs, that is, cancer-promoting CAFs (pCAF) and cancer-restraining CAFs (rCAF). Although various pCAF markers have been identified, the identity of rCAFs remains unknown because of the lack of rCAF-specific marker(s). In this study, we found that Meflin, a glycosylphosphatidylinositol-anchored protein that is a marker of mesenchymal stromal/stem cells and maintains their undifferentiated state, is expressed by pancreatic stellate cells that are a source of CAFs in pancreatic ductal adenocarcinoma (PDAC). *In situ* hybridization analysis of 71 human PDAC tissues revealed that the infiltration of Meflin-positive CAFs correlated with favorable patient outcome. Consistent herewith, Meflin deficiency led to significant tumor progression with poorly differentiated histology in a PDAC mouse model. Similarly, genetic ablation of Meflin-positive CAFs resulted in poor differentiation of tumors in a syngeneic transplantation model. Conversely, delivery of a Meflin-expressing lentivirus into the tumor stroma or overexpression of Meflin in CAFs suppressed the growth of xenograft tumors. Lineage tracing revealed that Meflin-positive cells gave rise to α-smooth muscle actin-positive CAFs that are positive or negative for Meflin, suggesting a mechanism for generating CAF heterogeneity. Meflin deficiency or low expression resulted in straightened stromal collagen fibers, which represent a signature for aggressive tumors, in mouse or human PDAC tissues, respectively. Together, the data suggest that Meflin is a marker of rCAFs that suppress PDAC progression.

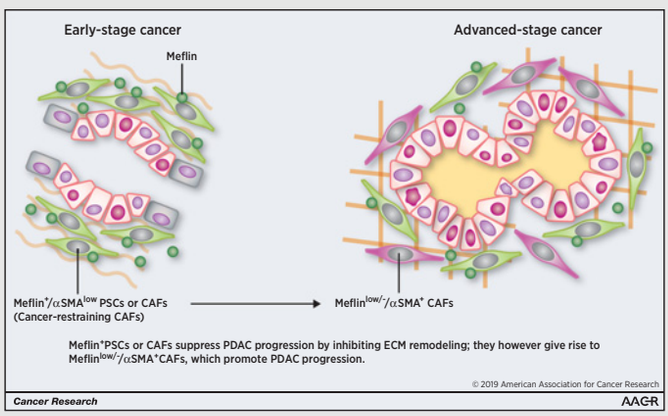

Significance: Meflin marks and functionally contributes to a subset of cancer-associated fibroblasts that exert antitumoral effects.
Graphical Abstract: http://cancerres.aacrjournals.org/content/canres/79/20/5367/F1.large.jpg.

[1]Department of Pathology, Nagoya University Graduate School of Medicine, Nagoya, Japan. [2]Department of Gastroenterology and Hepatology, Nagoya University Graduate School of Medicine, Nagoya, Japan. [3]School of Medicine, University of Adelaide and South Australian Health and Medical Research Institute, Adelaide, South Australia, Australia. [4]Division of Molecular Pathology, Center for Neurological Disease and Cancer, Nagoya University Graduate School of Medicine, Nagoya, Japan. [5]Division of Gastroenterology, Tohoku University Graduate School of Medicine, Sendai, Japan. [6]Faculty of Advanced Life Science, Hokkaido University, Sapporo, Japan. [7]Department of Cell and Regenerative Biology, University of Wisconsin-Madison, Madison, Wisconsin. [8]Division of Anatomy, Department of Human Development and Fostering, Meikai University School of Dentistry, Sakado, Japan. [9]Anatomy and Cell Biology, Nagoya University Graduate School of Medicine, Nagoya, Japan. [10]Division of Molecular Genetics, Shigei Medical Research Institute, Okayama, Japan. [11]Department of Surgery and Science, Graduate School of Medicine and Pharmaceutical Sciences, University of Toyama, Toyama, Japan. [12]Department of Gastroenterological Surgery (Surgery II), Nagoya University Graduate School of Medicine, Nagoya, Japan. [13]Division of Surgical Oncology, Department of Surgery, Nagoya University Graduate School of Medicine, Nagoya, Japan. [14]Division of Systems Biology, Nagoya University Graduate School of Medicine, Nagoya, Japan. [15]Department of Liver, Biliary Tract and Pancreas Diseases, Fujita Health University, Toyoake, Japan.

Note: Supplementary data for this article are available at Cancer Research Online (http://cancerres.aacrjournals.org/).

Y. Mizutani, H. Kobayashi, and T. Iida contributed equally to this article.

Corresponding Authors: Atsushi Enomoto, Nagoya University Graduate School of Medicine, 65 Tsurumai-cho, Showa-ku, Nagoya 466-8550, Japan. Phone: 81-52-744-2093; Fax: 81-52-744-2098; E-mail: enomoto@iar.nagoya-u.ac.jp; and Masahide Takahashi, mtakaha@med.nagoya-u.ac.jp

Cancer Res 2019;79:5367–81

doi: 10.1158/0008-5472.CAN-19-0454

Introduction

Tumors are not a homogenous mass of cancer cells, but also comprise many types of noncancer cells, including cancer-associated fibroblasts (CAF), myeloid cells, and lymphocytes (1, 2). These cells, together with tumor vessels and the extracellular matrix (ECM), shape the tumor microenvironment (TME), which is vital not only for the development and progression of cancer but also tumor immunity and resistance to anticancer therapies (1, 2).

CAFs constitute a major component of the TME and produce various types of ECM proteins, such as collagen, and soluble signaling molecules (3–8). CAFs promote the proliferation and invasion of cancer cells either directly via soluble signaling molecules or indirectly through the regulation of angiogenesis and immunity (3–9). Stromal fibrosis and stiffening driven by the ECM produced by CAFs, which are particularly conspicuous in aggressive cancers such as pancreatic ductal adenocarcinoma (PDAC), also increase cancer cell malignancy and therapeutic resistance (10–12). Many studies have shown positive correlations between CAF infiltration, monitored by analyzing standard CAF markers such as α-smooth muscle actin (αSMA), fibroblast-specific protein 1 (FSP1), fibroblast activation protein (FAP), and podoplanin, and poor outcome of patients with cancer (3, 4, 6, 8, 13–18). Thus, the biology of CAFs, including their origins, specific markers, functions, and clinical relevance, has gained increasing research interest in recent years (3–8). Clinical trials of therapeutics that target CAFs are also emerging, with investigations on the underlying mechanisms (4, 8, 19, 20).

One caveat in targeting CAFs, however, was pointed out by recent observations that the functions of individual CAFs are not necessarily the same (3–6, 8, 21–24). Genetic depletion of proliferating αSMA–positive (αSMA^+) CAFs and conditional blocking of the Sonic Hedgehog (Shh) signaling pathway, which is crucial for promoting desmoplasia in PDAC (25), led to the progression of PDAC in mouse models, suggesting that certain populations of CAFs, if not all, may function to suppress cancer progression (21–24). Clinical studies that evaluated the use of CAF inhibitors in patients with PDAC were not successful, raising the question whether CAFs promote or restrain cancer progression (12). The current view is that there exist heterogeneous populations of CAFs that comprise cancer-promoting CAFs (pCAF) and cancer-restraining CAFs (rCAF; refs. 3–6, 8). However, marker protein(s) that specifically label rCAFs have not been identified to date. As noted above, αSMA is a candidate marker of rCAFs (3, 12, 22). However, αSMA is widely expressed by pericytes, smooth muscle cells that form the tunica media of vessels, myoepithelial cells, and smooth muscle fibers of various organs, and thus, is not specific to CAFs (3, 5, 6). In addition, some studies have shown that αSMA expression in CAFs correlates with unfavorable prognosis in some types of cancer (15–18). Thus, the role of αSMA^+ CAFs in cancer progression remains controversial. Furthermore, it is unclear whether pCAFs and rCAFs represent distinct CAF populations with different origins or whether they undergo interconversion during tumor progression.

We previously identified Meflin, which is a glycosylphosphatidyl inositol (GPI)-anchored protein encoded by the immunoglobulin superfamily containing leucine-rich repeat (*ISLR*/*Islr*) gene, as a specific marker of mesenchymal stromal/stem cells (MSC) that are found in the perivascular space of multiple organs, including the bone marrow (BM; ref. 26). Meflin expression is limited to undifferentiated MSCs and is not detected in their differentiated lineages, such as mature osteoblasts, chondrocytes, and adipocytes (26). Forced overexpression of Meflin suppressed the expression of osteogenic and chondrogenic markers in an MSC cell line (26). Consistent with this, Meflin knockout (KO) resulted in accelerated osteoblastic differentiation of MSCs in the long bones. These data suggested that the primary function of Meflin is to maintain the undifferentiated state of MSCs (26). However, the histology of the other organs of Meflin-KO mice seemed to be indistinguishable from that of wild-type (WT) mice, leaving the role of Meflin in MSCs that exist throughout the body undetermined (26). A recent study revealed that Meflin is expressed by skeletal muscle stem cells and is crucial for skeletal muscle regeneration and the maintenance of the canonical Wnt signaling pathway (27). However, the mechanism underlying Meflin-mediated regulation of tissue stem cells remains to be precisely defined. It has been reported that Meflin interacts with disheveled segment polarity protein 2 (Dvl2), a cytoplasmic mediator of Wnt signaling (27). However, given that Meflin is a GPI-anchored cell-surface or -secreted protein, it is plausible that Meflin interacts with proteins in the lumen of the Golgi apparatus or with extracellular or membrane proteins.

In this study, we investigated the roles of Meflin and $Meflin^+$ cells in the development of PDAC. We first examined the expression pattern of Meflin in the normal pancreas and tumor tissues of human PDAC and its correlation with the clinical outcome. The significance of Meflin in PDAC progression was confirmed by experiments using Meflin-KO mice and a PDAC mouse model. Next, we analyzed the effect of genetic ablation of $Meflin^+$ cells on tumor progression and conducted a lineage-tracing experiment in mice. Then, we explored the molecular function of Meflin, and finally, investigated whether exogenous delivery of Meflin in the tumor stroma would suppress tumor development in mice.

Materials and Methods

Human tissue samples

Human PDAC samples were obtained at the time of surgery from patients who had provided written informed consent. This study was conducted in accordance with the Helsinki Declaration for Human Research and approved by the Ethics Committee of Nagoya University Graduate School of Medicine (approval number: 2017-0127).

Culture of cell lines and the isolation of human primary pancreatic stellate cells

Mouse PDAC cells (mT3, mT4, and mT5) were generously provided by David Tuveson (Cold Spring Harbor Laboratory) and Chang-Il Hwang (UC Davis College of Biological Sciences, Davis, CA). AsPC-1 and UE7T13 cells were purchased from the Japanese Cancer Research Resources Bank. U2OS, Saos-2, MBA-MB-231, and 578T cells were purchased from the ATCC. PANC-1, KLM-1, and KP-4 cells were obtained from the Cell Resource Center for Biomedical Research (Institute of Development, Aging, and Cancer, Tohoku University, Sendai, Japan). Cell lines were authenticated by routine morphologic and growth analyses. All cell lines were frozen at two passages and used in experiments

within five passages after thawing. All cell lines used were routinely screened for *Mycoplasma* contamination by 4′, 6-diamidino-2-phenylindole staining. Human pancreatic stellate cells (PSC) were isolated from pancreatic tissues adjacent to primary PDAC tumors during surgery at Tohoku University Hospital (28, 29). This study was approved by the Ethics Committees of Tohoku University (approval number 2017-1-280) and Nagoya University Graduate School of Medicine (approval number 2015-0254). Immortalized human PSCs were established by retrovirus-mediated introduction of the simian virus 40 (SV40) large T antigen (29).

Generation of gene-targeted mice and animal experiments, histology, cell biology, biochemistry, organoid culture, and statistical analysis

Animal protocols were approved by the Animal Care and Use Committee of Nagoya University Graduate School of Medicine (approval number: 30366). Detailed protocols for the generation of gene-targeted mice, *in situ* hybridization (ISH), IHC, cell biological, biochemical, and animal experiments and methods for statistical analysis are described in Supplementary Data.

Results

Meflin is a vitamin D–responsive marker of PSCs

We previously reported that Meflin is a marker of MSCs and is not expressed in pericytes, epithelial, endothelial, and smooth muscle cells, and blood and immune cells, and that it displays higher specificity for MSCs than other conventional MSC markers, such as CD90, CD105, and CD73 (26). Meflin$^+$ MSCs are found in the BM (Supplementary Fig. S1) and the perivascular regions of multiple organs, as shown in our previous study (26). This is consistent with the notion that MSCs localize in multiple tissues as perivascular fibroblasts (30). ISH analysis of mouse and human pancreases showed that few Meflin$^+$ cells are scattered in the perivascular, periductular, and periacinar regions (Fig. 1A and B). Meflin$^+$ cells were abundantly present in the early postnatal pancreas, but their number decreased in the adult stage (Supplementary Fig. S1). To confirm Meflin expression in the pancreas, we generated a Meflin reporter–knockin mouse model [Meflin-ZsGreen-diphtheria toxin receptor (DTR)-Cre recombinase (Meflin-ZDC)], in which the expression of a green fluorescent protein ZsGreen, DTR, and Cre was driven by the Meflin gene (*Islr*) promoter (Fig. 1C; Supplementary Fig. S2A–S2C). In the Meflin-ZDC mice, ZsGreen$^+$ cells expressed desmin (Fig. 1C), which is a known PSC marker (31). Immunofluorescence (IF) staining showed colocalization of Meflin and desmin at the protein level (Supplementary Fig. S1). These data suggested that Meflin is a new marker of PSCs. Meflin was expressed by PSCs isolated from the pancreas, which were positive for desmin but not for epithelial or endothelial markers, as indicated by Western blot analysis (Fig. 1D).

Consistent with our previous study on cultured MSCs (26), robust Meflin expression was observed in contact-inhibited PSCs cultured to a superconfluent monolayer, suggesting a shared mechanism for Meflin expression in MSCs and PSCs (Fig. 1E). PSC-specific expression of Meflin was also confirmed by the analysis of a recently published dataset of single-cell RNA sequencing (scRNA-seq) of healthy mouse pancreas, where Meflin was specifically detected in PSC populations but not in other cell populations (Supplementary Fig. S3A–S3C; ref. 32).

One of the hallmarks of PSCs is that they modulate their gene expression in response to vitamin D (33). A previous study that screened genes upregulated in PSCs treated with calcipotriol, a vitamin D analog, identified *Islr* as one of those genes (Supplementary Fig. S4A and S4B; ref. 33). Consistent herewith, most Meflin$^+$ spindle fibroblastic cells expressed the vitamin D receptor (VDR) within the pancreatic stroma of human PDAC (Fig. 1F). The coexpression of Meflin and VDR was also observed in the stroma of the KPC pancreatic cancer mouse model (Supplementary Fig. S5A and S5B; ref. 34). Calcipotriol-induced Meflin expression was also observed in cultured human and mouse PSCs, where 25-hydroxyvitamin D3-24-hydroxylase (*Cyp24A1*) served as a positive control of calcipotriol activity (Fig. 1G and H). Intriguingly, the expression of *Acta2*, which encodes αSMA, was downregulated by calcipotriol treatment in WT, but not Meflin-deficient PSCs (Fig. 1H). Calcipotriol-dependent Meflin expression was confirmed by a luciferase reporter assay with a vector containing the putative promoter region of the human Meflin gene (*ISLR*; Fig. 1I and J). Together, these data suggested that Meflin is a vitamin D–responsive PSC marker.

Meflin is a marker of CAFs in human PDAC and in a PDAC mouse model

Consistent with previous findings that PSCs are activated to become CAFs in PDAC (11, 33, 35–37), ISH analysis of human PDAC tissues revealed the presence of Meflin$^+$ cells in the proximity of invading cancer cells, even in small invasive lesions (Fig. 2A). In advanced PDAC cases, Meflin$^+$ cells were extensively distributed in the stroma of primary tumor lesions as well as in invasive lesions in peripancreatic adipose tissues (Fig. 2B). We also detected Meflin protein expression in stromal cells in some human PDAC samples by IHC using an anti-human Meflin mAb that we developed (Supplementary Fig. S6). However, IHC for Meflin often resulted in nonspecific staining of nonstromal cells that were negative for Meflin by ISH in other PDAC cases. Therefore, we adopted ISH to localize Meflin$^+$ cells throughout the study. Meflin expression was neither detected in cancer cells in human PDAC tissues nor PDAC cell lines (Figs. 1D, 2A, and B; Supplementary Figs. S6 and S7). A major fraction of the cells that were positive for platelet-derived growth factor receptor α (PDGFRα), an established fibroblast marker, was also positive for Meflin, suggesting that Meflin is a new marker of CAFs (Supplementary Fig. S8).

Interestingly, CAFs in human PDAC exhibited variable expression of Meflin and other conventional CAF markers. Notably, approximately 10% of CAFs expressing αSMA protein were positive for Meflin mRNA in human PDAC as determined by alkaline phosphatase–based IHC following ISH (Supplementary Fig. S8). Similarly, dual-color chromogenic ISH suggested that a small fraction of *ACTA2*-expressing cells expressed Meflin mRNA (Supplementary Fig. S9A). In line herewith, highly sensitive detection of αSMA and Meflin mRNAs by fluorescence ISH and quantification by counting the dots per cell revealed that CAFs strongly positive for Meflin were weakly positive for αSMA, and there was an inverse correlation between Meflin and αSMA expression (Supplementary Fig. S9B). These data suggested that Meflin and αSMA expression are not mutually exclusive; rather, Meflin$^+$ CAFs express a low level of αSMA.

Meflin was expressed by approximately 40% of FAP$^+$ CAFs (Supplementary Fig. S8) and by the majority of CAFs expressing

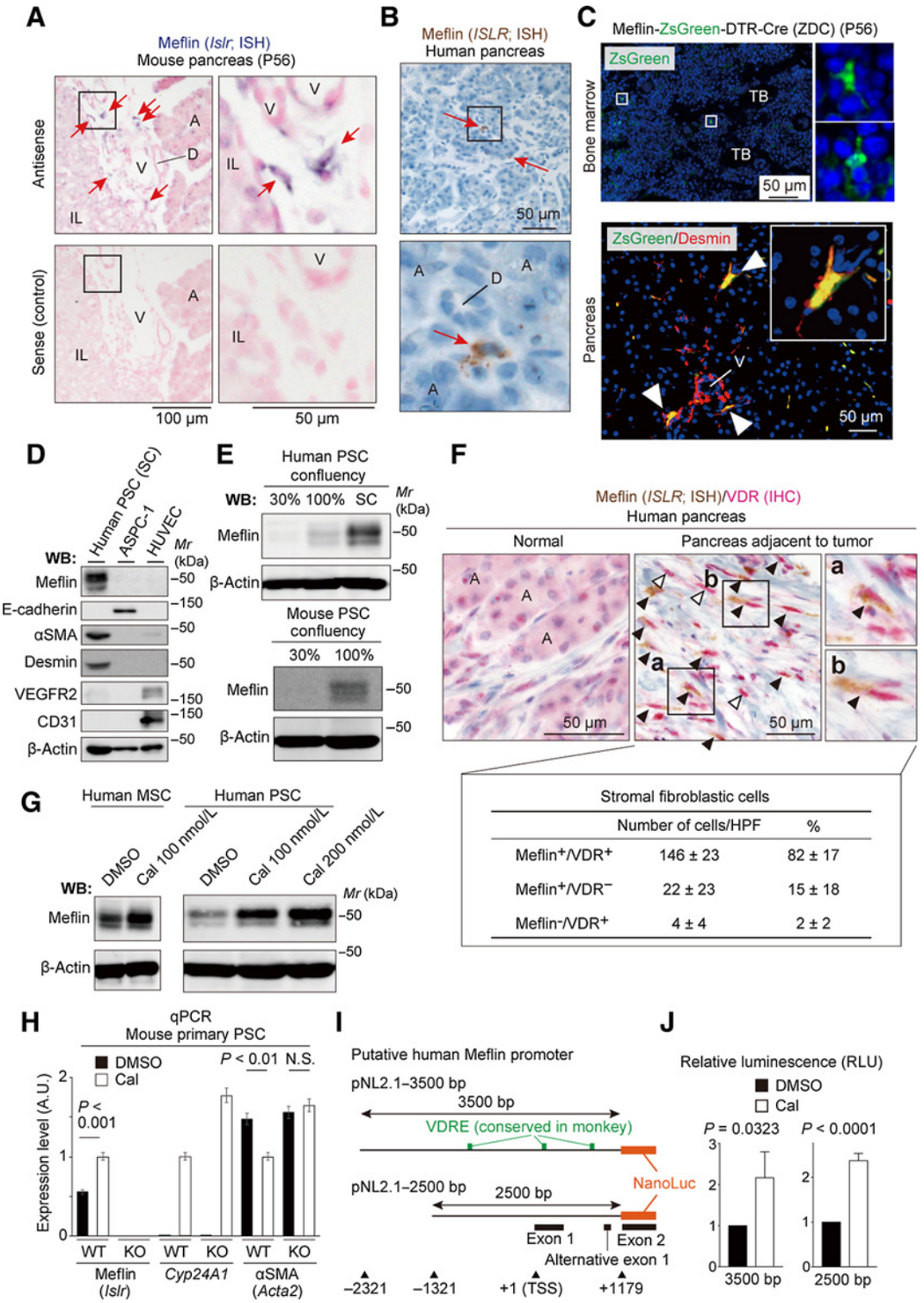

Figure 1.

Meflin is a vitamin D–responsive marker of PSCs. Meflin expression in the mouse (**A**) and human (**B**) pancreas was detected by ISH (arrows), followed by counterstaining with Kernechtrot stain solution and hematoxylin, respectively. The boxed areas are magnified in adjacent panels. V, vessel, A, acini, D, duct, IL, islet of Langerhans. **C,** Localization of ZsGreen$^+$ cells in the BM (top) and pancreas (bottom) of Meflin-ZDC mice. In the BM, ZsGreen$^+$ cells localized adjacent to the trabecular bones (TB) and sinusoids and the parenchyma of the BM. The boxed regions are magnified in adjacent panels or insets. In the pancreas, ZsGreen is coexpressed with desmin (red) in PSCs (arrowheads). V, vessel. **D,** Expression of desmin, but not epithelial and endothelial markers, in PSCs isolated from human pancreas and cultured to superconfluent (SC) monolayers. (*Continued on the following page.*)

Gli1, a transcription factor involved in the Shh pathway crucial for PDAC progression (Supplementary Fig. S8; refs. 12, 38). These data suggested that Meflin defines a population of CAFs that is αSMA^{low} $FAP^{+/-}$ $PDGFR\alpha^{+}$ $Gli1^{+}$ in human PDAC.

Meflin expression was also detected in tumors from KPC PDAC mice (Fig. 2C). $Meflin^{+}$ CAFs appeared in the early stage of acinar-to-ductal metaplasia and were present in greater numbers in the preinvasive lesion of the developed tumor, where rare αSMA^{+} CAFs were present in close proximity to p53 strongly positive cancer cells, and in the invasive front of the invasive lesion (Fig. 2C). Meflin expression was not detected in cancer cells throughout the tumorigenic process (Fig. 2C and D; Supplementary Fig. S7). As observed in human PDAC tissues, Meflin and αSMA expression are inversely correlated when analyzed at the mRNA level by fluorescence ISH, providing additional support for the finding that CAFs strongly positive for Meflin are weakly positive for αSMA (Fig. 2E and F). The inverse correlation between Meflin and αSMA expression in CAFs was also confirmed by the analysis of publicly available datasets of scRNA-seq analysis of CAFs isolated from the KPC model and a breast cancer mouse model (Fig. 2G; Supplementary Figs. S10 and S11; refs. 36, 39). The data showed that the CAF population that is highly positive for Meflin is distinct from populations enriched for αSMA and the PSC marker desmin.

Meflin expression in CAFs correlates with favorable outcome of human patients with PDAC and KPC mice

Next, we assessed the effect of alterations in Meflin expression on global gene expression profiles in MSCs, a potential source of CAFs (8), using a gene expression microarray (Supplementary Fig. S12A–S12C). The data showed that Meflin depletion resulted in the upregulation of cytokines such as IL6 and C-C motif chemokine ligand 2 (CCL2) and several markers of activated CAFs, such as αSMA and Gli1. Furthermore, gene set enrichment analysis demonstrated the upregulation of previously reported activated PSC signature genes in Meflin-depleted MSCs (Supplementary Fig. S12D; ref. 33). These data suggested that alterations in Meflin expression in CAFs may be involved in gene expression changes associated with CAF activation.

When we investigated Meflin expression in surgically resected human PDAC tissues ($N = 71$), we found that the frequency of $Meflin^{+}$ CAFs varies between patients with PDAC (Fig. 3A; Supplementary Table S1). We evaluated the number and ratio of $Meflin^{+}$ cells in total stromal cells (visualized by hematoxylin counterstaining), excluding cells with the morphology of lymphocytes, erythrocytes, and endothelial cells. We divided the 71 cases into Meflin-high ($\geq$20% $Meflin^{+}$ stromal cells) and Meflin-low (<20% $Meflin^{+}$ stromal cells) groups (Fig. 3A; Supplementary Table S1). The Meflin-high group exhibited better prognosis in Kaplan–Meier survival analysis and a more differentiated histology than the Meflin-low group, suggesting a unique feature of $Meflin^{+}$ CAFs that is distinct from that of previously described pCAFs, which correlates with poor outcome (Fig. 3B; Supplementary Tables S1 and S2).

As we previously reported, Meflin-KO mice exhibit slight growth retardation and accelerated growth of long bones in the postnatal stages, but become indistinguishable from WT mice as they grow into young adults (26). These mice are viable and fertile, with grossly normal pancreatic tissue (Supplementary Fig. S13A and S13B). However, we found that tumors that developed in compound transgenic Meflin-KO KPC mice were significantly larger and more proliferative than those developed in WT KPC mice (Fig. 3C–F; Supplementary Fig. S13C and S13D), which was consistent with the poorer survival rate of Meflin-KO mice than that of WT mice (Fig. 3G). Reflecting the higher tumor burden with more necrosis in Meflin-KO KPC mice, the number of apoptotic cells was marginally but significantly increased in Meflin-KO KPC tumors compared with that in WT KPC tumors (Fig. 3F). These data further supported the notion that Meflin functionally defines a CAF population that is distinct from conventional pCAFs.

Meflin suppresses poor differentiation of PDAC

Further histologic analyses revealed that tumors in Meflin-KO KPC model mice were poorly differentiated compared with tumors in WT KPC mice (Fig. 4A and B). Meflin-KO tumors contained more αSMA^{+} CAFs and more collapsed tumor vessels than WT tumors (Fig. 4C and D). These data suggested that the loss of Meflin led to increased αSMA expression in CAFs and decreased tumor vessel perfusion. The expression of FAP, a marker of pCAFs (8, 11), was not significantly different between WT and Meflin-KO KPC tumors (Supplementary Fig. S13E and S13F). Next, organoids established from KPC tumors developed in Meflin-KO mice were orthotopically transplanted into the pancreases of WT and Meflin-KO mice (Fig. 4E). Histologic analysis showed that the tumors engrafted into WT pancreas exhibited features of well-differentiated tumors, with an acinar-like appearance, whereas those engrafted and developed in KO pancreas exhibited features of poorly differentiated tumors (Fig. 4E and F). These data suggested that Meflin shapes the TME, which blocks poor differentiation in PDAC.

Genetic ablation of $Meflin^{+}$ CAFs results in poor differentiation of subcutaneously transplanted tumors

To investigate the role of $Meflin^{+}$ CAFs in tumor differentiation further, we subcutaneously transplanted syngeneic mT5 PDAC cells (40) into Meflin-ZDC; Rosa26-LSL (LoxP-stop-LoxP)-tdTomato mice, followed by intratumoral administration of diphtheria toxin to ablate cells that actively express Meflin (Fig. 5A). ISH

(*Continued.*) ASPC-1, a human PDAC cell line; HUVEC, human umbilical vein endothelial cell. **E,** PSCs isolated from human and mouse pancreases were cultured to 30% and 100% confluence or as superconfluent monolayers, followed by Western blot (WB) analysis. *Mr*, molecular marker. **F,** Normal pancreas and pancreatic tissue adjacent to PDAC were double stained for Meflin (ISH, brown) and VDR (IHC, red). Ten high-power fields (HPF, 400×) were randomly selected from three patients and were histologically evaluated. $Meflin^{+}/VDR^{+}$ fibroblastic cells and $Meflin^{-}/VDR^{+}$ cells are labeled by solid and open arrowheads, respectively. Numbers of single- or double-positive cells in pancreas tissue adjacent to the tumor are indicated in the table in the bottom panel. Representative double-positive cells are magnified in adjacent panels (**a** and **b**). Note that acinar cells are also positive for VDR. A, acini. **G** and **H,** Human primary cultured MSCs and PSCs were treated with DMSO or calcipotriol (Cal) at the indicated concentrations for 48 hours, followed by Western blot analysis (**G**) and qPCR (**H**). N.S, not significant; A.U, arbitrary unit. **I** and **J,** Human Meflin putative promoter regions 3500 or 2500 bp upstream from the start point of exon 2 [−2321 or −1321 to +1179; +1 is the transcription start site (TSS)] were ligated to a NanoLuc reporter gene (**I**) and transfected into human PSCs, followed by either DMSO or calcipotriol treatment for 48 hours and the measurement of luciferase activity (**J**). VDRE, putative vitamin D–responsive element.

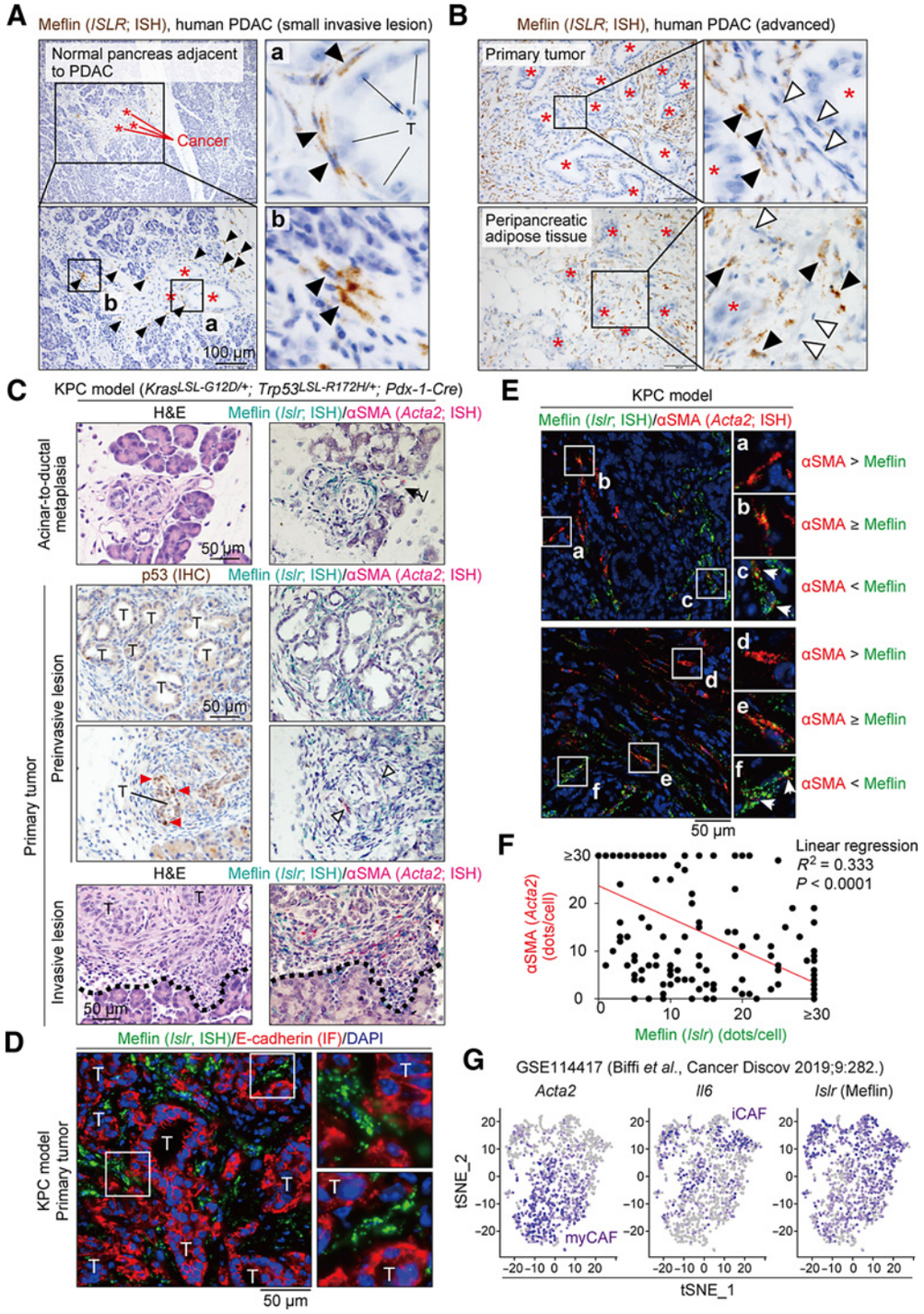

Figure 2.

Meflin is expressed by a subpopulation of CAFs of human and mouse PDAC. **A,** Infiltration of Meflin$^+$ CAFs (brown, arrowheads) in the proximity of invading cancer glands (asterisks) in a small invasive lesion of human PDAC. The boxed areas (**a** and **b**) are magnified in adjacent panels. T, tumor cells. **B,** Infiltration of Meflin$^+$ CAFs in the primary tumor region (top) or the tumor invading the peripancreatic adipose tissue (bottom) of an advanced human PDAC case. Note that Meflin$^+$ stromal cells (solid arrowheads) and Meflin-negative stromal cells (open arrowheads) coexisted in the same sample. Asterisks, cancer cell glands that are negative for Meflin. **C,** Meflin (*Islr*; green) and αSMA (*Acta2*; red) expression in mouse PDAC tissues was examined by ISH. Meflin$^+$ cells infiltrated the tissue around lesions of the acinar-to-ductal metaplasia, which is known to develop into precancerous pancreatic intraepithelial neoplasia in the KPC model, where αSMA$^+$ CAFs were not yet detected (top). In PDAC tissues, Meflin$^+$ CAFs were extensively distributed throughout the tumor stroma, where αSMA$^+$ cells were sparsely present around cancer cells overexpressing p53 (red arrowheads; middle). (*Continued on the following page.*)

analysis showed that endogenous Meflin was successfully depleted in tumors developed in diphtheria toxin–injected mice (Fig. 5B and C). The tumors depleted of Meflin$^+$ cells exhibited no apparent changes in volume; however, they possessed a higher proliferative capacity and more poorly differentiated histology than tumors developed in the control groups (Fig. 5D–G). These data implied that Meflin$^+$ CAFs include some CAF populations that block poor tumor differentiation. Furthermore, we found that the ablation of Meflin$^+$ CAFs led to a decrease in the αSMA$^+$ area (Fig. 5H and I), suggesting that Meflin$^+$ CAFs might be involved in the infiltration or recruitment of αSMA$^+$ CAFs into the tumor stroma. Alternatively, αSMA$^+$ CAFs might be derived from Meflin$^+$ CAFs during tumor progression.

Meflin$^+$ cells yield αSMA$^+$ CAFs in a xenograft tumor model

To investigate whether Meflin$^+$ CAFs yield αSMA$^+$ CAFs *in vivo*, we generated a knockin mouse line in which the expression of a fusion protein of the Cre recombinase and the mutated ligand-binding domain of the human estrogen receptor (CreERT2) was driven by the Meflin (*Islr*) promoter (Meflin-CreERT2; Supplementary Fig. S14A and S14B). We generated Meflin-CreERT2; Rosa26-LSL-tdTomato mice to trace the lineage of Meflin$^+$ cells by tamoxifen administration. Tamoxifen administration induced the expression of tdTomato in BM MSCs that are located around the trabecular bones, arterioles, periosteum, and sinusoids, as well as in PSCs with long cytoplasmic processes in the pancreas, supporting the notion that Meflin is a marker of these cells (Supplementary Fig. S14C and S14D). We subcutaneously transplanted syngeneic mT3 PDAC cells (40) following a 2-week washout period after tamoxifen administration (Fig. 6A). Meflin$^+$ cells gave rise to 34% ± 15% of all αSMA$^+$ CAFs on day 10 after transplantation (Fig. 6B). ISH analysis revealed that the number of tdTomato$^+$ Meflin-lineage cells that expressed αSMA, but not those that expressed FAP, significantly increased between day 3 (46% ± 26%) and day 10 (93% ± 4%; Fig. 6C–F). Moreover, 42% ± 4% and 58% ± 4% ($P = 0.0427$) of tdTomato$^+$ Meflin-lineage cells had lost endogenous Meflin expression on day 3 and day 10, respectively (Fig. 6G and H). These data suggested that Meflin$^+$ cells yield CAFs that are positive for αSMA$^+$, and negative or positive for Meflin.

Exogenous expression of Meflin suppresses tumor progression in a xenograft tumor model

Our previous study showed that forced overexpression of Meflin suppressed the expression of the osteoblast and chondrocyte differentiation markers in MSCs (26). Therefore, we hypothesized that exogenous expression of Meflin would suppress the myofibroblastic phenotype of CAFs and influence the TME and tumor progression. Exogenous Meflin expression suppressed αSMA expression in cultured MSCs (Supplementary Fig. S15), which was consistent with the observation that Meflin expression suppressed the capacity of MSCs to contract a collagen matrix (Fig. 7A–C). The ability of MSCs to form colony-forming unit fibroblasts (CFU-F) was also enhanced by Meflin expression, consistent with the role of Meflin in maintaining the undifferentiated state of MSCs (Fig. 7D and E; ref. 26). Subcutaneous xenografts comprising of AsPC-1 PDAC cells and immortalized human PSCs (29) transduced with Meflin exhibited tumor growth regression and decreased infiltration of αSMA$^+$ CAFs compared with AsPC-1 cell and control human PSC xenografts in immunodeficient mice (Supplementary Fig. S16A–S16F). Furthermore, we engineered mT3 PDAC cells to produce lentiviruses that could infect surrounding stromal cells and implanted these cells into C57BL/6 mice (Fig. 7F–I). Transplantation of mT3 cells expressing a lentivirus encoding Meflin increased Meflin expression in the tumor stroma, which was accompanied by the suppression of tumor growth and αSMA$^+$ CAF infiltration when compared with control mT3 cells expressing a lentivirus encoding the green fluorescent protein Azami Green. These data suggested that the transduction of Meflin into tumor tissues or the augmentation of Meflin expression in CAFs may provide a strategy to suppress tumor progression.

Meflin is involved in the regulation of stromal collagen structure

Finally, given our recent finding that Meflin is expressed in cardiac fibroblasts and suppresses cardiac fibrosis and stiffening of cardiac tissue in a chronic heart failure mouse model (41), we explored the involvement of Meflin in stromal collagen structural remodeling by second-harmonic generation (SHG) microscopic observations of WT and Meflin-KO KPC tumors (Fig. 7J–L; Supplementary Fig. S17A–S17C). The data revealed that the stroma of tumors developed in Meflin-KO KPC mice exhibited straighter and wider collagen structures than that of tumors in WT KPC mice. Differences in collagen signature such as altered curvature, total length, density, and alignment of fibers were observed between Meflin-high (≥20% stromal cells were positive for Meflin) and -low areas of the stroma of human PDAC tissues based on SHG measurements (Supplementary Fig. S17D–S17J). Given the significance of changes in collagen configuration in cancer progression (42–44), these data suggested that Meflin suppresses tumor progression in part by inhibiting the remodeling collagen structure (Fig. 7M).

(*Continued.*) At the invasive front of tumors, αSMA$^+$ CAFs infiltrated as much as Meflin$^+$ CAFs (bottom). Each image in the right column represents a serial section of the sample immediately following the section shown on the left. V, vessel; T, tumor. **D,** A paraffin-embedded tissue section from a mouse KPC tumor sample was stained with mouse Meflin (*Islr*)-specific probe by ISH (green), followed by staining for E-cadherin by IF (red). Meflin expression is not detectable in cancer cells. The boxed areas are magnified in the adjacent panels. T, tumor glands. **E,** Inverse correlation between Meflin and αSMA expression in CAFs infiltrating tumors in KPC mice. Meflin (*Islr*; green) and αSMA (*Acta2*; red) expression in tumors in KPC mice was examined by duplex ISH with custom fluorescence RNAscope probes. The boxed areas (**a–f**) are magnified in adjacent panels. Arrows indicate the presence of a few dots representing weak αSMA expression in Meflin$^+$ CAFs. CAFs exhibit variable levels of Meflin and αSMA expression, with an inverse correlation between Meflin and αSMA expression in CAFs in the stroma of PDAC in KPC mice. **F,** ISH results shown in **E** were quantified following a semiquantitative scoring method, where the expression of Meflin and αSMA was evaluated on the basis of the number of dots per cell. Cells with more than 30 dots were collectively classified as "≥30." All scoring was performed at a magnification of ×400 for 164 randomly selected cells in the tumor sample. Simple linear regression analysis showed an inverse correlation ($R^2 = 0.333$; $P < 0.0001$) between Meflin and αSMA expression. **G,** t-distributed stochastic neighbor embedding (t-SNE) plot showing CAF subpopulations (*Il6*-positive iCAF and *Acta2*-positive myCAF), which were identified by scRNA-seq of all cells isolated from tumors of the KPC mouse model of PDAC (GEO accession code GSE114417). Each dot is a CAF, and the intensity of the purple represents the expression level of the indicated genes. The iCAF and myCAF populations of CAFs were defined by Biffi and colleagues (36). See also Supplementary Fig. S10.

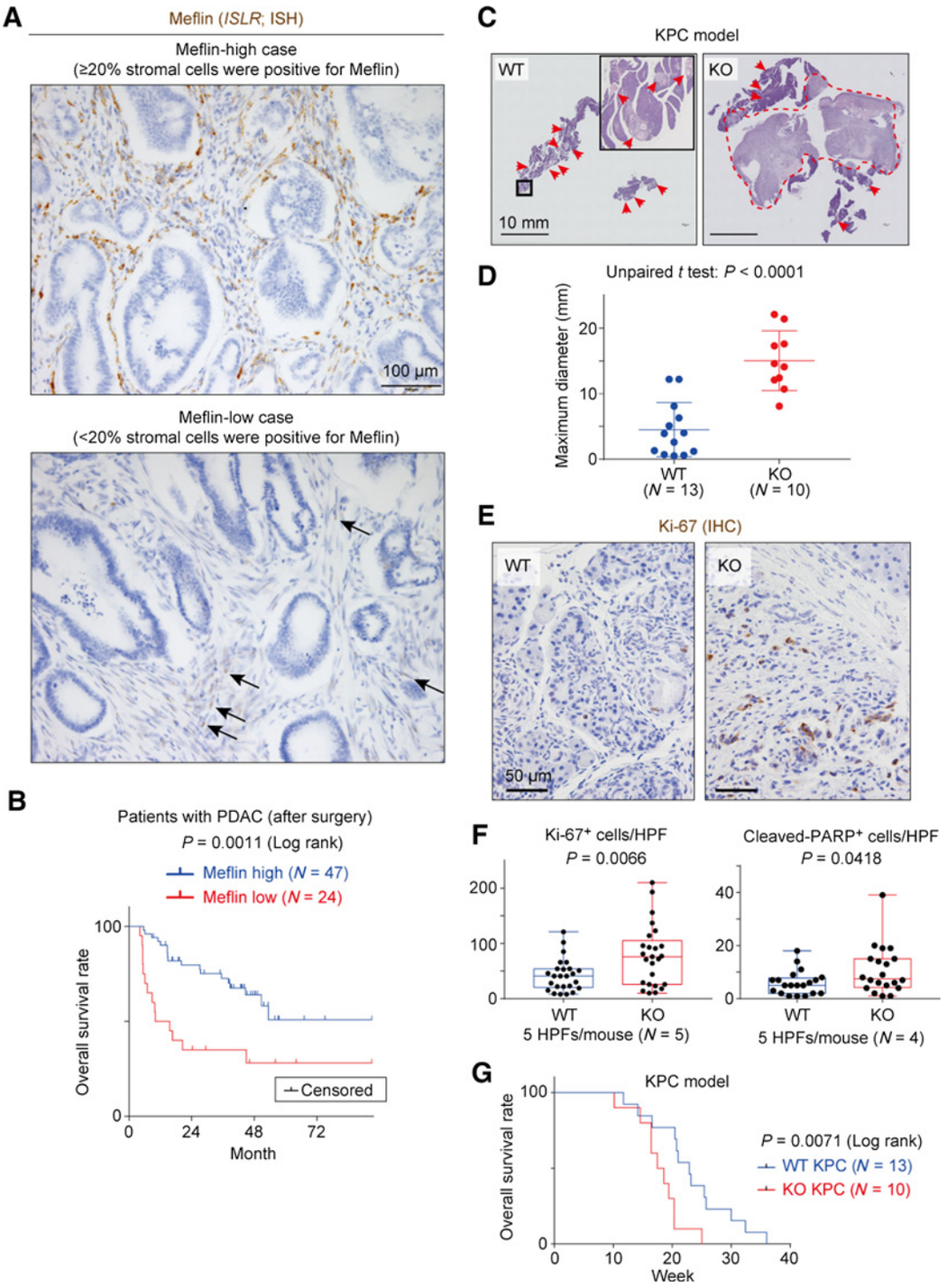

Figure 3.

Meflin expression in CAFs correlates with favorable outcome of PDAC in human and mice. **A,** Representative ISH images of Meflin-high (top) and Meflin-low (bottom) cases. Cases with Meflin$^+$ cells accounting for more than 20% of all stromal fibroblast–like cells were considered Meflin-high cases. In the Meflin-low case shown in the bottom panel, cells weakly positive for Meflin (arrows) were observed but represented less than 20% of total stromal fibroblast–like cells. **B,** Overall survival rates of patients with PDAC postsurgery for the Meflin-high and Meflin-low groups. **C,** Representative hematoxylin and eosin-stained sections of tumors from WT and Meflin-KO mice crossed with KPC pancreatic cancer model mice. Arrowheads and the dotted line indicate the developed tumors. The boxed area in the WT tumor is magnified in the inset. **D,** Maximum diameters of the largest tumors developed in WT and Meflin-KO KPC mice. **E** and **F,** Sections of tumors developed in WT and Meflin-KO KPC mice were stained with anti-Ki-67 and anti-cleaved PARP antibodies to detect proliferative and apoptotic cells, respectively, and the positive cells per high-power field (400×) were counted. **G,** Survival rates of WT KPC and Meflin-KO KPC mice.

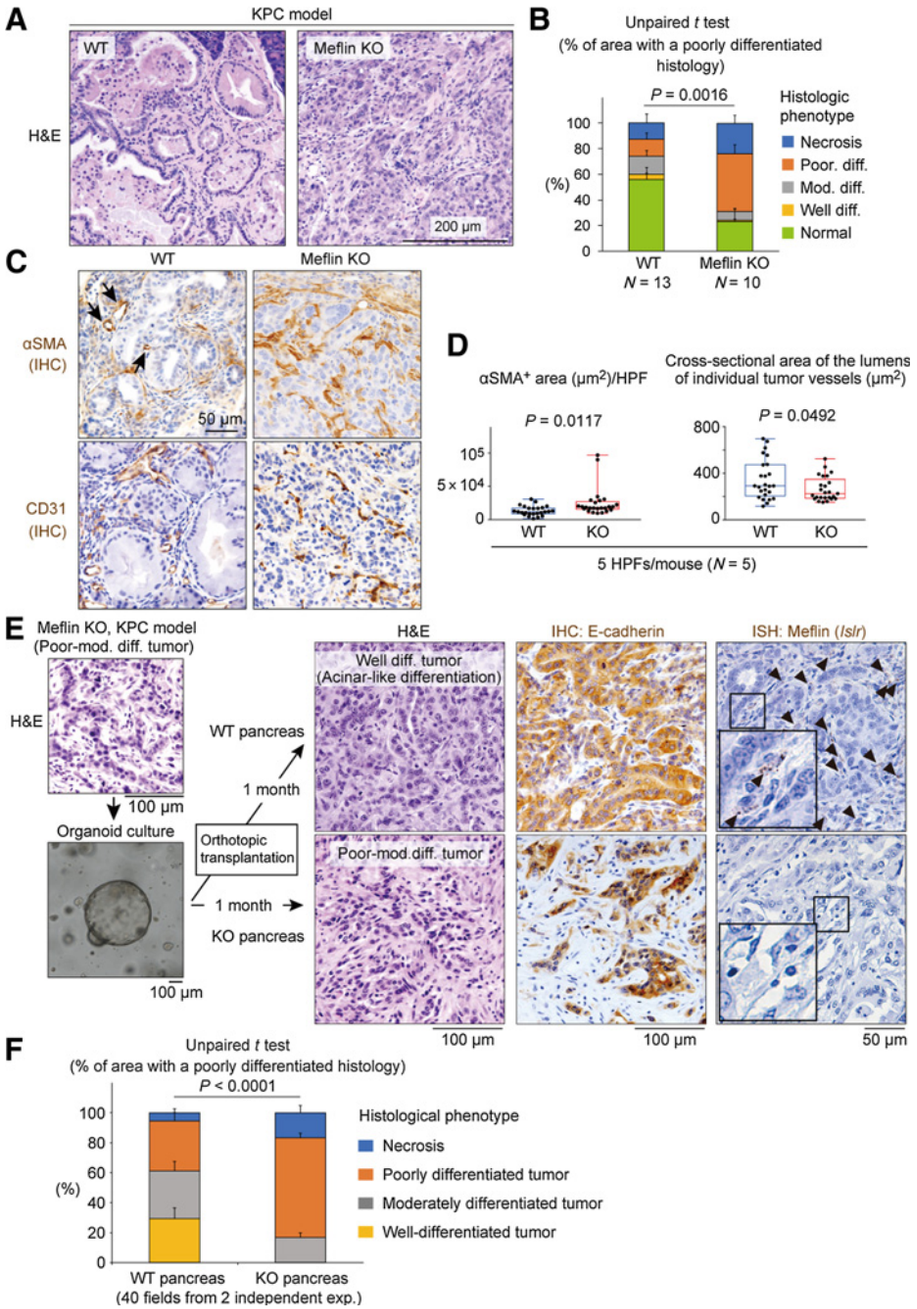

Figure 4.

Meflin modifies the TME that restrains poor differentiation of PDAC in mice. **A,** Representative hematoxylin and eosin (H&E)-stained sections of tumors developed in WT (left) and Meflin-KO (right) KPC mice. Note that tumors in KO mice were poorly differentiated compared with those in WT mice. **B,** Histologic phenotype of tumors in WT and Meflin-KO KPC mice. Ten high-power field (HPF; 400×) were randomly selected from 5 mice in each group for histologic evaluation. The sum total area of each differentiation type was expressed relative to the area of the pancreas. Mod, moderately; poor, poorly. **C** and **D,** Tissue sections from WT and Meflin-KO KPC mice were stained for αSMA and CD31. The αSMA^{+} area per HPF and the cross-sectional area of the lumens of individual $CD31^{+}$ tumor vessels were measured and quantified. Arrows in **C** indicate αSMA expression in the walls of tumor vessels, but not in CAFs. **E** and **F,** Orthotopic transplantation of KPC tumor cells grown in organoid culture into the pancreases of WT and Meflin-KO mice. Tumors developed in Meflin-KO KPC mice were dissected and grown in three-dimensional organoid culture using Intesticult Organoid Growth Medium. The organoids were transplanted into the pancreases of WT (top, right) and Meflin-KO (bottom, right) mice. **E,** Representative hematoxylin and eosin-, E-cadherin (IHC)-, and Meflin (ISH)-stained images of the developed tumors harvested 1 month after transplantation. Tumors developed in the pancreases of WT mice exhibited a well-differentiated pattern that contained acinar-like structures, whereas those developed in the pancreases of Meflin-KO mice were poorly or moderately differentiated. **F,** Evaluation of the histologic phenotypes of the developed tumors after orthotopic transplantation. Thirty HPFs (400×) were randomly selected from 2 mice in each group for histologic evaluation. The sum total area of each differentiation type was expressed relative to the area occupied by the entire tumor.

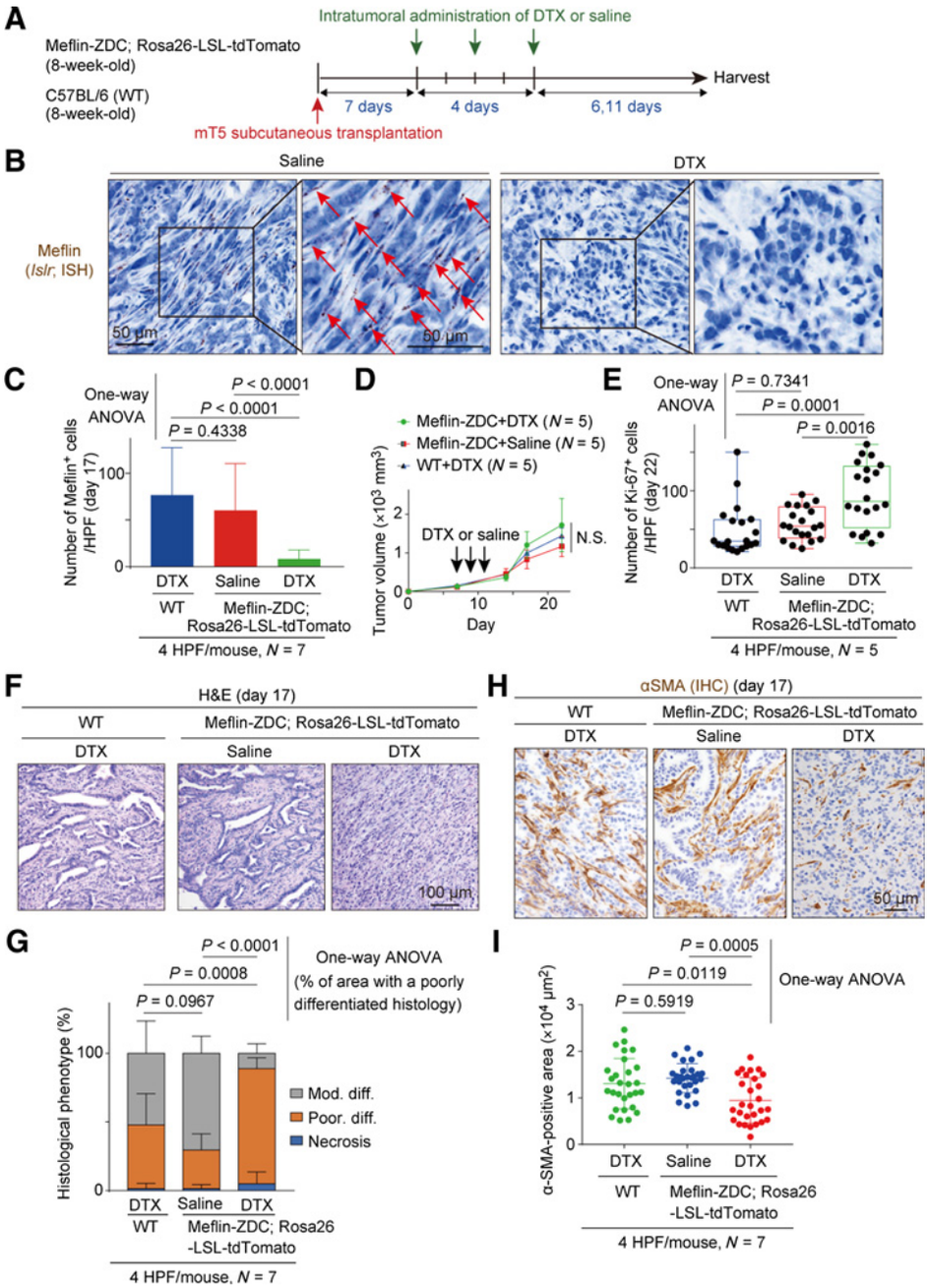

Figure 5.

Genetic ablation of Meflin$^+$ CAFs results in poorly differentiated tumors using a subcutaneous model. **A,** Meflin-ZDC; Rosa26-LSL-tdTomato mice (P56) were subcutaneously transplanted with mT5 mouse PDAC cells (5×10^6 cells/mouse), followed by intratumoral administration of either diphtheria toxin (DTX; 10 μg/kg) to ablate Meflin$^+$ cells or normal saline as a control. Treatments were performed three times. To assess possible adverse effects of diphtheria toxin administration, C57BL/6 WT mice were subjected to the same treatments. Tissues were harvested 17 days after transplantation and histologically analyzed. Tumor sections were stained for endogenous Meflin by ISH (**B**), followed by quantification (**C**). The data showed depletion of Meflin$^+$ CAFs in tumors administered with diphtheria toxin (bottom), but not in those administered with saline (top). **D,** Tumor sizes. **E,** Ki-67$^+$ cells in tissue sections of tumors in the indicated groups were counted and quantified. **F,** Representative hematoxylin and eosin (H&E)-stained sections of tumors administered saline or diphtheria toxin in control or Meflin-ZDC; Rosa26-LSL-tdTomato mice. Note that tumors administered diphtheria toxin in Meflin-ZDC; Rosa26-LSL-tdTomato mice exhibited a more poorly differentiated histology. **G,** Histologic evaluation of subcutaneous tumors developed in mice after intratumoral administration of saline or diphtheria toxin. Four randomly selected high-power field (HPF; 400×) from each mouse (7 mice per group) were evaluated by two independent pathologists blinded to the treatments. **H,** Representative images of αSMA IHC in tumors administered saline or diphtheria toxin in control (WT) or Meflin-ZDC; Rosa26-LSL-tdTomato mice. **I,** Quantification of αSMA–positive areas in tumors in each group. Four randomly selected HPFs (400×) from each mouse (7 mice in each group) were evaluated using ImageJ software.

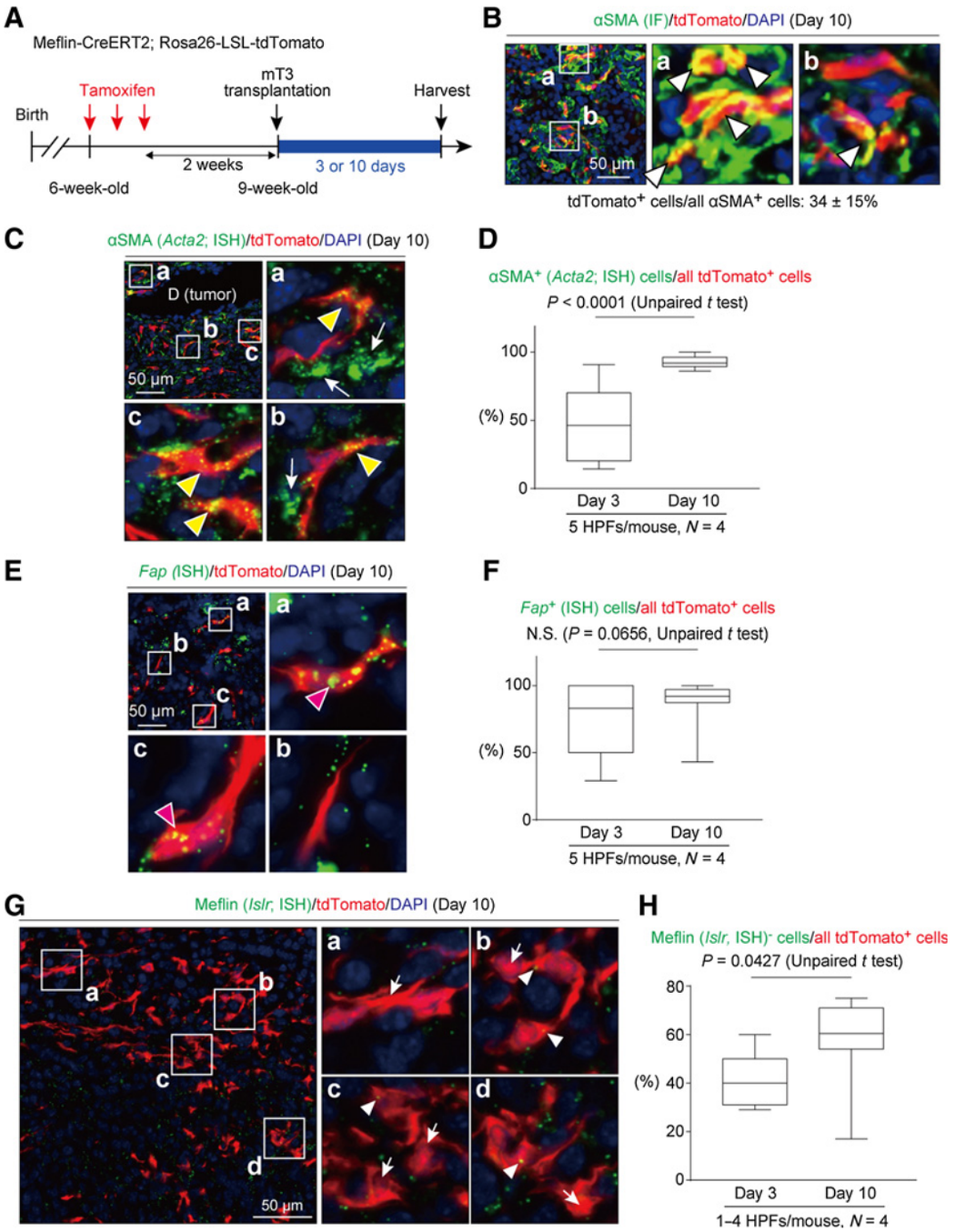

Figure 6.

Lineage tracing of Meflin$^+$ cells during tumor development. Meflin-CreERT2; Rosa26-LSL-tdTomato mice were administered tamoxifen (0.1 mg/g) three times with a 2-week washout period before the subcutaneous transplantation of mT3 mouse PDAC cells, tissue harvesting (**A**), IF for αSMA (**B**), and ISH for αSMA and FAP (**C–F**). The boxed areas are magnified in adjacent panels. The IF data showed that some tdTomato$^+$ Meflin-lineage cells were positive for αSMA protein expression (open arrowheads). The ISH data showed that tdTomato$^+$ Meflin-lineage cells yielded weakly αSMA$^+$ CAFs (yellow arrowheads), but not strongly αSMA$^+$ CAFs (arrows) and FAP$^+$ CAFs (magenta arrowheads; **C** and **E**). In **D** and **F**, αSMA and FAP positivity determined by ISH in tdTomato$^+$ Meflin-lineage cells were quantified. Five high-power fields (400×) randomly selected from four mice were analyzed and quantified. D, ducts of the transplanted tumor. **G** and **H,** Approximately half of Meflin-lineage CAFs became negative for endogenous Meflin expression during tumor development. ISH analysis showed that 42% ± 4% and 58% ± 4% of tdTomato$^+$ Meflin-lineage cells were negative for endogenous Meflin (arrows) on day 3 and day 10, respectively, suggesting that approximately half of Meflin-lineage cells became Meflin-negative during tumor progression. Representative images of tdTomato$^+$ cells in tumor tissues on day 10 are shown. Arrowheads denote Meflin-lineage cells that were positive for endogenous Meflin. The boxed areas (**a–d**) are magnified in adjacent panels. In **H**, Meflin negativity determined by ISH in tdTomato$^+$ Meflin-lineage cells was quantified. One to four sections (400×) randomly selected from four mice were analyzed and quantified.

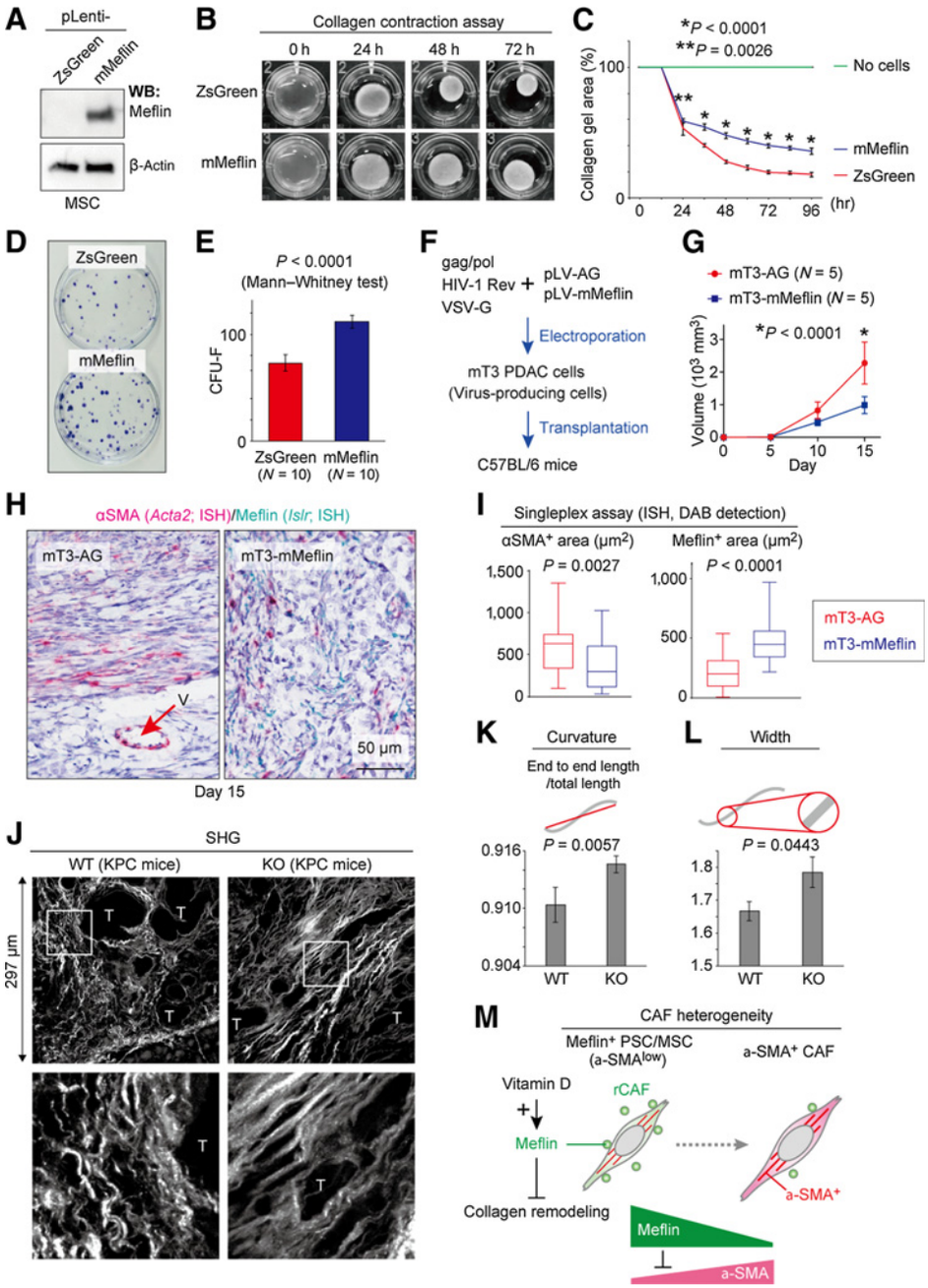

Figure 7.

Meflin inhibits the myofibroblastic phenotype of cultured MSCs and αSMA expression in CAFs of xenografted mouse tumors, and modulates collagen architecture. **A–C,** Lentivirus-mediated transduction of mouse Meflin (mMeflin) suppressed the capacity of mouse MSCs to contract collagen gels. Statistical significance was assessed using two-way ANOVA followed by Bonferroni *post hoc* correction ($N = 4$ in each group). **D** and **E,** Lentivirus-mediated transduction of mMeflin restored CFU-F formation in mouse MSCs. **F–I,** Scheme of subcutaneous transplantation of syngeneic mT3 cells that were engineered to produce lentiviruses expressing the green fluorescent protein Azami Green and mMeflin into C57BL/6 mice (**F**). **G,** Tumor volumes after transplantation. The infiltration of αSMA^+ and $Meflin^+$ CAFs was examined by ISH (**H**), followed by quantification of the αSMA^+ and $Meflin^+$ areas (**I**). Thirty randomly selected high-power fields from 5 mice in each group were evaluated. In **G**, statistical significance was assessed using two-way ANOVA followed by Bonferroni *post hoc* correction. **J–L,** Measurement of collagen alignment in the stroma of tumors developed in WT and Meflin-KO KPC mice by SHG microscopy. Three randomly selected images from tissue sections of WT ($N = 6$) and Meflin-KO ($N = 6$) KPC tumors were analyzed. Representative images (**J**) and quantification of collagen straightness (curvature; **K**) and width (**L**) are shown. The boxed areas are magnified in the bottom panels. T, tumor. **M,** Working hypothesis for CAF heterogeneity and its role in PDAC progression. Our data suggest that Meflin expression defines a subset of rCAFs, inhibiting the remodeling of the stromal collagen structure to shape the cancer-restraining TME. $Meflin^+$ rCAFs, which may originate from PSCs or MSCs, differentiate into αSMA^+ CAFs that are negative or weakly positive for Meflin. Meflin expression is induced by vitamin D, the clinical significance of which merits further investigation.

Discussion

It was first suggested over 50 years ago that the primary function of normal fibroblasts is to inhibit the growth of polyoma virus–transformed cells (45). Consistent with this landmark study, the presence of rCAFs in the TME has been postulated on the basis of the findings that genetic ablation of proliferating αSMA$^+$ cells and genetic and pharmacologic inhibition of Shh signaling promoted cancer progression in mouse models of PDAC (22–24). However, the role of αSMA$^+$ CAFs in cancer progression is controversial, and the precise nature of rCAFs has not been defined (3, 8, 11, 13, 15–18, 22). In this study, we showed that in the healthy pancreas, Meflin marks PSCs, whose relationship with MSCs had not been fully explored previously. Meflin also marks a population of CAFs in PDAC, with high Meflin expression correlating with favorable outcome in patients with PDAC and a PDAC mouse model. Meflin functions to suppress PDAC progression, presumably by suppressing αSMA expression in CAFs and changing collagen configuration in the tumor stroma. A lineage-tracing experiment showed that Meflin-lineage cells contained αSMA$^+$ CAFs, some of which exhibited downregulated Meflin expression. Taking all data into consideration, we speculate that Meflin is a marker of rCAFs (αSMA^{low} PDGFRα$^+$ Gli1$^+$), which yield αSMA$^+$ Meflin$^{low/-}$ CAFs during PDAC progression. Given that CAFs expressing high levels of Meflin express low levels of αSMA, it is speculated that genetic depletion of Meflin$^+$ CAFs also resulted in depletion of a subset of proliferating αSMA$^+$ CAFs that were previously reported to have a cancer-restraining action (22).

In this study, the mechanisms underlying the downregulation of Meflin expression in CAFs remains to be unraveled. We previously reported that repeated passage and long-term culture of primary MSCs on cell culture plastic induced a significant decrease or loss in Meflin expression, in which the stiffness of their substrate is crucial (26). Immortalization of MSCs and human PSCs also resulted in the loss of Meflin expression. Other factors that significantly downregulate Meflin expression include aging, hypoxia, and transforming growth factor-β signaling, which has been shown to induce differentiation of PSCs into αSMA$^+$ myofibroblastic CAFs (myCAF; refs. 41, 36). We speculate that some of these factors are involved in the downregulation of Meflin expression in Meflin$^+$ PSCs and CAFs, which results in the generation of Meflin-negative or weakly positive CAFs and thus contributes to the generation of CAF heterogeneity during tumor progression. Recently, two distinct populations of CAFs derived from quiescent PSCs were identified in the tumor stroma of mouse PDAC, that is, αSMA$^+$ myCAFs and IL6$^+$ inflammatory CAFs (iCAF; refs. 12, 35, 36). Transcriptome analysis of these cells revealed that Meflin is expressed, in descending order, in quiescent PSCs (basemean value 2623.5), iCAFs (basemean value 665.7), and myCAFs [basemean value 125.0; Gene Expression Omnibus (GEO) accession no. GSE93313; ref. 35]. Further studies are needed to clarify the exact interrelationships between iCAFs, myCAFs, and Meflin$^+$ CAFs. We have not yet determined whether Meflin$^+$ CAFs originate from quiescent Meflin$^+$ PSCs in the pancreas *in vivo*, it is possible that they are also derived from Meflin$^+$ MSCs in the BM and other organs. Another limitation of this study is that we evaluated Meflin expression by ISH, not IHC; thus, how Meflin proteins are distributed in the tumor stroma and whether they act on non-CAFs, including tumor cells, remains to be resolved.

One interesting finding in this study was that PDAC that developed in Meflin-KO mice was poorly differentiated. This was confirmed by orthotopic transplantation of mouse PDAC organoids into the pancreases of WT and Meflin-KO mice and genetic ablation of Meflin$^+$ CAFs in a xenograft tumor model. Given that Meflin is not expressed by pancreatic acini, ducts, the islets of Langerhans, vessels, blood cells, or tumor cells, the data support the notion that CAF phenotypes determine the behavior and differentiation of tumor cells. This is also supported by previous studies showing that depletion of proliferating αSMA$^+$ CAFs or inhibition of the Shh pathway yielded predominantly undifferentiated tumor cells in mouse models of PDAC (22, 23). These findings are compatible with the concept that the TME influences the malignant phenotype, and a high degree of plasticity of differentiation status in cancer cells exists within tumors (7, 46–48). The detailed mechanisms of Meflin-mediated alterations of the tumor stroma have not been clarified in this study, but one potential explanation based on SHG observations of WT and Meflin-KO KPC tumors is that Meflin may be involved in the suppression of the activity of the lysyl oxidase (Lox) family of proteins and excessive ECM cross-linking. Considering the involvement of Lox activity in increased stiffness of the tumor stroma that is crucial for the activation of cancer cells and cancer progression (42–43), it will be interesting to investigate the role of Meflin in the regulation of the mechanical properties of the tumor stroma in future studies.

We also showed that exogenous expression of Meflin in the tumor stroma suppressed αSMA expression in CAFs and tumor progression. It is, therefore, tempting to investigate whether it would be possible to reverse the phenotype of pCAFs by restoring Meflin expression and to suppress cancer progression. In this respect, it was interesting to find that most Meflin$^+$ cells found in the pancreas adjacent to PDAC were positive for VDR and that Meflin expression was upregulated by vitamin D. These data are consistent with the findings in previous studies that vitamin D or A treatments restored a quiescent state in PSCs, suppressed inflammation and fibrosis of the tumor stroma of PDAC, and increased tumor sensitivity to gemcitabine (12, 33, 49, 50). These studies have provided a rationale for the use of vitamin D analogs in combination with either chemotherapy or immune checkpoint inhibitors for the treatment of patients with PDAC in clinical trials (e.g., clinicaltrials.gov, NCT03331562 and NCT03519308). A critical issue that warrants a further investigation is how varied Meflin expression in CAFs is involved in the response of human PDAC to those combined treatments.

In conclusion, we found that Meflin is a marker of PSCs in the normal pancreas. Consistent with previous studies showing that PSCs can be activated to become CAFs in PDAC, Meflin expression was detected in CAFs in the tumor stroma of both human PDAC and a PDAC mouse model. Interestingly, Meflin expression in CAFs correlated with favorable outcomes in human PDAC and the mouse model. We also showed that Meflin has the capacity to suppress αSMA expression (myofibroblastic differentiation) in CAFs and ECM remodeling, which is crucial for cancer progression. Together, our data suggest that Meflin is a marker of a subpopulation of rCAFs in PDAC.

Disclosure of Potential Conflicts of Interest

No potential conflicts of interest were disclosed.

Authors' Contributions

Conception and design: Y. Mizutani,, H. Kobayashi, Y. Hirooka, A. Enomoto, M. Takahashi

Development of methodology: Y. Mizutani, H. Kobayashi, T. Iida, L. Weng, M. Matsuyama, T. Kobayashi

Acquisition of data (provided animals, acquired and managed patients, provided facilities, etc.): Y. Mizutani, H. Kobayashi, T. Iida, N. Asai, A. Hara, N. Esaki, S. Mii, K. Ando, S. Ishihara, S.M. Ponik, M.W. Conklin, T. Miyata, M. Matsuyama, T. Kobayashi, T. Fujii, S. Yamada, A. Enomoto

Analysis and interpretation of data (e.g., statistical analysis, biostatistics, computational analysis): Y. Mizutani, H. Kobayashi, T. Iida, Y. Shiraki, S. Ishihara, S.M. Ponik, M.W. Conklin, T. Fujii, T. Wang, D. Worthley, T. Shimamura, A. Enomoto, M. Takahashi

Writing, review, and/or revision of the manuscript: Y. Mizutani, H. Kobayashi, S. Ishihara, S.M. Ponik, H. Haga, A. Nagasaka, T. Fujii, S.L. Woods, D. Worthley, Y. Hirooka, A. Enomoto, M. Takahashi

Administrative, technical, or material support (i.e., reporting or organizing data, constructing databases): N. Asai, A. Masamune, K. Ushida, H. Haga, A. Nagasaka, M. Matsuyama, T. Kobayashi, J. Yamaguchi

Study supervision: D. Worthley, M. Fujishiro, Y. Hirooka, A. Enomoto, M. Takahashi

Acknowledgments

We thank Patricia J. Keely (University of Wisconsin-Madison, Madison, WI), who sadly passed away in 2017, for her support in SHG microscopy; David Tuveson (Cold Spring Harbor Laboratory) and Chang-Il Hwang (UC Davis College of Biological Sciences, Davis, CA) for providing the mouse PDAC cell lines mT3, mT4, and mT5; Genichiro Ishii and Yasuhiro Matsumura (National Cancer Center), Masahiro Sokabe and Hiroyoshi Nishikawa (Nagoya University, Nagoya, Japan), Akira Orimo (Juntendo University, Tokyo, Japan), Satoru Kidoaki (Kyushu University, Fukuoka, Japan), Takashi Okada and Yoshiyuki Yamazaki (Nippon Medical School, Tokyo, Japan), Takuya Kato (Kitasato University, Tokyo, Japan), and Yumi Matsuzaki (Shimane University, Matsue, Japan) for helpful discussions; Kentaro Taki (Nagoya University, Nagoya, Japan) for help with mass spectrometry; Toshiro Sato (Keio University, Tokyo, Japan) for technical assistance in organoid culture; Takeshi Urano (Shimane University, Matsue, Japan) for technical assistance in protein purification; and Kozo Uchiyama (Nagoya University, Nagoya, Japan) for technical assistance. This work was supported by a Grant-in-Aid for Scientific Research (S) (26221304 to M. Takahashi) and a Grant-in-Aid for Scientific Research (B) (15H04719 and 18H02638 to A. Enomoto, and 15H04804 and 19H03631 to A. Masamune) commissioned by the Ministry of Education, Culture, Sports, Science and Technology of Japan; Nagoya University Hospital Funding for Clinical Research (to A. Enomoto); The Hori Sciences And Arts Foundation (to A. Enomoto); Kobayashi Foundation for Cancer Research (to A. Enomoto); AMED-CREST (Japan Agency for Medical Research and Development, Core Research for Evolutional Science and Technology; to A. Enomoto and H. Haga); the Project for Cancer Research and Therapeutic Evolution (P-CREATE) from AMED (to A. Enomoto); the Mochida Memorial Foundation for Medical and Pharmaceutical Research (to A. Enomoto); and the Smoking Research Foundation (to A. Masamune). H. Kobayashi is supported by the Japan Society for the Promotion of Science (JSPS) Overseas Challenge Program for Young Researchers and Takeda Science Foundation Fellowship.

The costs of publication of this article were defrayed in part by the payment of page charges. This article must therefore be hereby marked *advertisement* in accordance with 18 U.S.C. Section 1734 solely to indicate this fact.

Received February 5, 2019; revised June 17, 2019; accepted August 1, 2019; published first August 22, 2019.

References

1. Hanahan D, Coussens LM. Accessories to the crime: functions of cells recruited to the tumor microenvironment. Cancer Cell 2012;21:309–22.
2. Chen DS, Mellman I. Elements of cancer immunity and the cancer-immune set point. Nature 2017;541:321–30.
3. Kalluri R. The biology and function of fibroblasts in cancer. Nat Rev Cancer 2016;16:582–98.
4. Chen X, Song E. Turning foes to friends: targeting cancer-associated fibroblasts. Nat Rev Drug Discov 2019;18:99–115.
5. Öhlund D, Elyada E, Tuveson D. Fibroblast heterogeneity in the cancer wound. J Exp Med 2014;211:1503–23.
6. Ishii G, Ochiai A, Neri S. Phenotypic and functional heterogeneity of cancer-associated fibroblast within the tumor microenvironment. Adv Drug Deliv Rev 2016;99:186–96.
7. Bissell MJ, Hines WC. Why don't we get more cancer? A proposed role of the microenvironment in restraining cancer progression. Nat Med 2011;17:320–9.
8. Kobayashi H, Enomoto A, Woods SL, Burt AD, Takahashi M, Worthley D. Cancer-associated fibroblasts in gastrointestinal cancer. Nat Rev Gastroenterol Hepatol 2019;16:282–95.
9. Costa A, Kieffer Y, Scholer-Dahirel A, Pelon F, Bourachot B, Cardon M, et al. Fibroblast heterogeneity and immunosuppressive environment in human breast cancer. Cancer Cell 2018;33:463–479.
10. Northey JJ, Przybyla L, Weaver VM. Tissue force programs cell fate and tumor aggression. Cancer Discov 2017;7:1224–1237.
11. Neesse A, Algül H, Tuveson DA, Gress TM. Stromal biology and therapy in pancreatic cancer: a changing paradigm. Gut 2015;64:1476–84.
12. Neesse A, Bauer CA, Öhlund D, Lauth M, Buchholz M, Michl P, et al. Stromal biology and therapy in pancreatic cancer: ready for clinical translation? Gut 2019;68:159–171.
13. Yuzawa S, Kano MR, Einama T, Nishihara H. PDGFRβ expression in tumor stroma of pancreatic adenocarcinoma as a reliable prognostic marker. Med Oncol 2012;29:2824–30.
14. Kawase A, Ishii G, Nagai K, Ito T, Nagano T, Murata Y, et al. Podoplanin expression by cancer associated fibroblasts predicts poor prognosis of lung adenocarcinoma. Int J Cancer 2008;123:1053–9.
15. Fujita H, Ohuchida K, Mizumoto K, Nakata K, Yu J, Kayashima T, et al. α-Smooth muscle actin expressing stroma promotes an aggressive tumor biology in pancreatic ductal adenocarcinoma. Pancreas 2010;39:1254–1262.
16. Sinn M, Denkert C, Striefler JK, Pelzer U, Stieler JM, Bahra M, et al. α-Smooth muscle actin expression and desmoplastic stromal reaction in pancreatic cancer: results from the CONKO-001 study. Br J Cancer 2014;111:1917–23.
17. Valach J, Fík Z, Strnad H, Chovanec M, Plzák J, Cada Z, et al. Smooth muscle actin-expressing stromal fibroblasts in head and neck squamous cell carcinoma: increased expression of galectin-1 and induction of poor prognosis factors. Int J Cancer 2012;131:2499–508.
18. Underwood TJ, Hayden AL, Derouet M, Garcia E, Noble F, White MJ, et al. Cancer-associated fibroblasts predict poor outcome and promote periostin-dependent invasion in oesophageal adenocarcinoma. J Pathol 2015;235:466–77.
19. Purcell JW, Tanlimco SG, Hickson J, Fox M, Sho M, Durkin L, et al. LRRC15 is a novel mesenchymal protein and stromal target for antibody-drug conjugates. Cancer Res 2018;78:4059–72.
20. Poggi A, Varesano S, Zocchi MR. How to hit mesenchymal stromal cells and make the tumor microenvironment immunostimulant rather than immunosuppressive. Front Immunol 2018;9:262.
21. Gore J, Korc M. Pancreatic cancer stroma: friend or foe? Cancer Cell 2014;25:711–712.
22. Özdemir BC, Pentcheva-Hoang T, Carstens JL, Zheng X, Wu CC, Simpson TR, et al. Depletion of carcinoma-associated fibroblasts and fibrosis induces immunosuppression and accelerates pancreas cancer with reduced survival. Cancer Cell 2014;25:719–34.
23. Rhim AD, Oberstein PE, Thomas DH, Mirek ET, Palermo CF, Sastra SA, et al. Stromal elements act to restrain, rather than support, pancreatic ductal adenocarcinoma. Cancer Cell 2014;25:735–747.
24. Lee JJ, Perera RM, Wang H, Wu DC, Liu XS, Han S, et al. Stromal response to Hedgehog signaling restrains pancreatic cancer progression. Proc Natl Acad Sci U S A 2014;111:E3091–E3100.
25. Bailey JM, Swanson BJ, Hamada T, Eggers JP, Singh PK, Caffery T, et al. Sonic hedgehog promotes desmoplasia in pancreatic cancer. Clin Cancer Res 2008;14:5995–6004.

26. Maeda K, Enomoto A, Hara A, Asai N, Kobayashi T, Horinouchi A, et al. Identification of Meflin as a potential marker for mesenchymal stromal cells. Sci Rep 2016;6:22288.
27. Zhang K, Zhang Y, Gu L, Lan M, Liu C, Wang M, et al. Islr regulates canonical Wnt signaling-mediated skeletal muscle regeneration by stabilizing dishevelled-2 and preventing autophagy. Nat Commun 2018;9:5129.
28. Masamune A, Kikuta K, Watanabe T, Satoh K, Hirota M, Hamada S, et al. Fibrinogen induces cytokine and collagen production in pancreatic stellate cells. Gut 2009;58:550–9.
29. Hamada S, Masamune A, Takikawa T, Suzuki N, Kikuta K, Hirota M, et al. Pancreatic stellate cells enhance stem cell-like phenotypes in pancreatic cancer cells. Biochem Biophys Res Commun 2012;421:349–354.
30. El Agha E, Kramann R, Schneider RK, Li X, Seeger W, Humphreys BD, et al. Mesenchymal stem cells in fibrotic disease. Cell Stem Cell 2017;21:166–177.
31. Apte M, Haber P, Applegate T, Norton I, McCaughan G, Korsten M, et al. Periacinar stellate shaped cells in rat pancreas: identification, isolation, and culture. Gut 1998;43:128–133.
32. Tabula Muris Consortium. Single-cell transcriptomics of 20 mouse organs creates a Tabula Muris. Nature 2018;562:367–372.
33. Sherman MH, Yu RT, Engle DD, Ding N, Atkins AR, Tiriac H, et al. Vitamin D receptor-mediated stromal reprogramming suppresses pancreatitis and enhances pancreatic cancer therapy. Cell 2014;159:80–93.
34. Hingorani SR, Wang L, Multani AS, Combs C, Deramaudt TB, Hruban RH, et al. Trp53R172H and KrasG12D cooperate to promote chromosomal instability and widely metastatic pancreatic ductal adenocarcinoma in mice. Cancer Cell 2005;7:469–83.
35. Öhlund D, Handly-Santana A, Biffi G, Elyada E, Almeida AS, Ponz-Sarvise M, et al. Distinct populations of inflammatory fibroblasts and myofibroblasts in pancreatic cancer. J Exp Med 2017;214:579–596.
36. Biffi G, Oni TE, Spielman B, Hao Y, Elyada E, Park Y, et al. IL-1-induced JAK/STAT signaling is antagonized by TGF-beta to shape CAF heterogeneity in pancreatic ductal adenocarcinoma. Cancer Discov 2018;9:282–301.
37. Apte MV, Wilson JS, Lugea A, Pandol SJ. A starring role for stellate cells in the pancreatic cancer microenvironment. Gastroenterology 2013;144:1210–9.
38. Thayer SP, di Magliano MP, Heiser PW, Nielsen CM, Roberts DJ, Lauwers GY, et al. Hedgehog is an early and late mediator of pancreatic cancer tumorigenesis. Nature 2003;425:851–6.
39. Bartoschek M, Oskolkov N, Bocci M, Lövrot J, Larsson C, Sommarin M, et al. Spatially and functionally distinct subclasses of breast cancer-associated fibroblasts revealed by single cell RNA sequencing. Nat Commun 2018;9:5150.
40. Boj SF, Hwang CI, Baker LA, Chio II, Engle DD, Corbo V, et al. Organoid models of human and mouse ductal pancreatic cancer. Cell 2015;160:324–38.
41. Hara A, Kobayashi H, Asai N, Saito S, Higuchi T, Kato K, et al. Roles of the mesenchymal stromal/stem cell marker Meflin in cardiac tissue repair and the development of diastolic dysfunction. Circ Res 2019;125:414–30.
42. Barker HE, Cox TR, Erler JT. The rationale for targeting the LOX family in cancer. Nat Rev Cancer 2012;12:540–552.
43. Levental KR, Yu H, Kass L, Lakins JN, Egeblad M, Erler JT, et al. Matrix crosslinking forces tumor progression by enhancing integrin signaling. Cell 2009;139:891–906.
44. Provenzano PP, Eliceiri KW, Campbell JM, Inman DR, White JG, Keely PJ. Collagen reorganization at the tumor-stromal interface facilitates local invasion. BMC Med 2006;4:38.
45. Stoker MG, Shearer M, O'Neill C. Growth inhibition of polyoma-transformed cells by contact with static normal fibroblasts. J Cell Sci 1966;1:297–310.
46. Weaver VM, Petersen OW, Wang F, Larabell CA, Briand P, Damsky C, et al. Reversion of the malignant phenotype of human breast cells in three-dimensional culture and in vivo by integrin blocking antibodies. J Cell Biol 1997;137:231–45.
47. Park CC, Bissell MJ, Barcellos-Hoff MH. The influence of the microenvironment on the malignant phenotype. Mol Med Today 2000;6:324–9.
48. Bissell MJ, Labarge MA. Context, tissue plasticity, and cancer: are tumor stem cells also regulated by the microenvironment? Cancer Cell 2005;7:17–23.
49. Froeling FE, Feig C, Chelala C, Dobson R, Mein CE, Tuveson DA, et al. Retinoic acid-induced pancreatic stellate cell quiescence reduces paracrine Wnt-β-catenin signaling to slow tumor progression. Gastroenterology 2011;141:1486–97.
50. Chronopoulos A, Robinson B, Sarper M, Cortes E, Auernheimer V, Lachowski D, et al. ATRA mechanically reprograms pancreatic stellate cells to suppress matrix remodelling and inhibit cancer cell invasion. Nat Commun 2016;7:12630.